Guo Yunlong (Orcid ID: 0000-0002-4490-2140)

Physical Aging of PS Blocks under 3D Soft Confinement in PS-*b*-PnBMA Diblock Copolymer: Two Equilibrations on The Way

Mingchao Ma[1] and Yunlong Guo*[,1,2]

[1]University of Michigan – Shanghai Jiao Tong University Joint Institute, and [2]School of Materials Science and Engineering, Shanghai Jiao Tong University, Shanghai 200240, China

*Corresponding author, E-mail: yunlong.guo@sjtu.edu.cn

Table of Contents

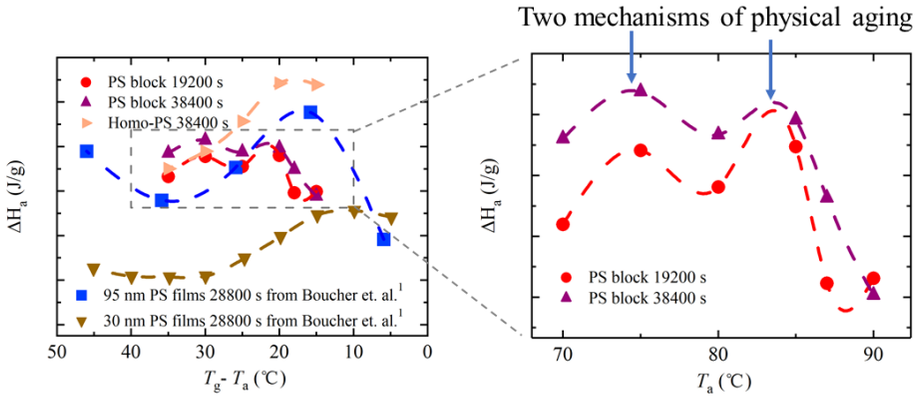

Two local maximums of T_a-dependent ΔH_a of PS block in PS-*b*-PnBMA indicate two relaxation mechanisms during physical aging.

Abstract

Polystyrene-*block*-poly(n-butyl methacrylate) (PS-*b*-PnBMA) was used to investigate three-dimensional (3D) soft confinement effect on physical aging of the PS block therein. The soft confinement is constructed by phase-separated PnBMA domains, as PnBMA is liquid on the aging temperatures of PS blocks due to its low glass transition temperature. In enthalpy recovery, aging response of PS blocks is represented by a low and broad heat capacity peak associated with an enhanced aging rate with respect to homo-PS, when the aging temperature is relatively low. However, the aging response exhibits opposite characteristics at relatively

This is the author manuscript accepted for publication and has undergone full peer review but has not been through the copyediting, typesetting, pagination and proofreading process, which may lead to differences between this version and the Version of Record. Please cite this article as doi: 10.1002/pol.29921

high temperatures, compared with the results of homo-PS. The phase-separated morphology and thus the soft confinement on PS blocks was confirmed by AFM imaging using the Peak Force QNM technique. Two local maximums of recovered enthalpy versus aging temperature indicate that two equilibration processes exist during aging of confined PS blocks, within a substantially shorter timescale to the bulk. The 3D soft confinement effect on aging of PS blocks is attributed to dual equilibration mechanisms: one dominates at higher aging temperatures, leading to a restrained aging rate, while the other plays a key role at lower aging temperatures, resulting in accelerated physical aging.

1 Introduction

Upon rapidly cooling from liquids, glass-forming materials including polymers enter their glassy states out of equilibrium. Owing to constrained molecular mobility, polymers slowly get close to equilibrium when annealed at a temperature below the glass transition temperature (T_g). During the process of approaching equilibrium, many physical properties, such as modulus,[4-6] enthalpy,[7-9] gas permeability[10-12] and dielectric property,[13-15] change with time and temperature. This evolution is referred as physical aging or structure relaxation.[17-19] Physical aging has attracted much attention in the last several decades,[20-22] as the understanding of its behavior and associated mechanism can provide indispensable knowledge for the better application of polymeric materials.

In recent years, some works showed that physical aging process might not only involve a unique equilibration mechanism.[23-30] For instance, it was demonstrated for several polymers that the relaxed enthalpy after a prolonged isothermal aging reached a plateau higher than the equilibrium value determined from extrapolated liquid line.[23-25] Moreover, Roth and coworkers reported that polystyrene (PS) thin films exhibited two distinct T_gs, indicating two simultaneous mechanisms in structural recovery.[26] Recently, Cangialosi *et al.* provided direct evidence of the two equilibrations by carefully monitoring enthalpy relaxation of PS and polycarbonate (PC).[27] Their results manifested two legible enthalpy recovery steps in sequence during the aging up to two years, in which the second recovery plateau approached the extrapolated liquid line.[27] Similarly, step-wise relaxation processes were also detected in metallic glasses[28-29] and arsenic selenide glasses[30]. Nevertheless, Simon and coworkers called into question the validity of two equilibrations in enthalpy recovery.[31] They did not observe the secondary plateau higher than the extrapolated liquid line after an aging for sufficiently long.[31] The validity of the two equilibrations in physical aging need to be further elucidated.

Physical aging is dramatically influenced by molecular mobility. As such, physical properties in aging process, such as enthalpy and fictive temperature (*i.e.*, the temperature corresponding

to the intersection of extrapolated glass and liquid lines for a specific glass, denoted as T_f), are noticeably different under confinement, since the mobility of confined polymer chains remarkably deviate from the bulk. The two equilibrations were demonstrated in polymers under confinement, *e.g.*, soft confined PS and poly(4-*tert*-butyl styrene) (PtBS).[1, 32-34]

As naturally double edged, aging rate depends on the thermodynamic driving force of structural relaxation and the enthalpy span between the initial and equilibrium points, in which the former increases with higher temperature, while the latter has a negative correlation with increase of temperature. Enthalpy relaxation or T_f should has a single local extreme point over aging temperature (T_a), after aged for a certain period. However, Boucher and coworkers revealed that recovered enthalpy of PS thin films under confinement showed two distinguishing local maximums in a regime of aging temperature, after aged for 28,800 s (480 min).[1, 32] In addition, Perez-De-Eulate *et al.* exposited two local minimums of T_f versus T_a in PS nanospheres after aged for 3,600 s (60 min).[33] These reports suggest the existence of the second (a fast process, see below) mechanism of relaxation in nanoconfined polymeric systems, by examining the profile of T_f versus T_a. A notable finding in these works is that the second plateau of PS films or nanospheres was detected within 28,800 s,[1, 33] which is much shorter than the time of two years for bulk PS,[27] showing much reduced timescale for the presence of the second equilibration due to soft confinement. Despite recent progress suggesting the existence of two equilibrations in confined polymers, systematical investigation is insufficient to date. The generality and underlying mechanism for such two equilibrations are not well understood.

Here we report physical aging of PS under 3D soft confinement in block copolymers. Block copolymers are of technological importance in drug delivery,[35-37] photovoltaics,[38-40] nanolithography,[41-43] *etc*. The typical applications of copolymers in glassy state could be bottlenecked due to lack of knowledge of physical aging under confinement. It is recently recognized that diblock copolymer is an ideal model material to study 3D confinement as the components confine each other by microphase separation.[3, 44-46] In this article, a PS-*b*-PnBMA diblock copolymer is utilized to investigate physical aging of the PS block under soft

confinement. The PnBMA block has a fairly low T_g, so that it is in liquid state at the typical aging temperatures of the PS block, forming soft confinement by phase separation. We present there are two local maximums of relaxed enthalpy (ΔH_a) of the PS block, as a function of T_a after aged for a certain period within 38,400 s. To the best of our knowledge, it is the first report on the two equilibrations during physical aging of block copolymers.

2 Experimental Section

2.1 Materials

The PS-*b*-PnBMA diblock copolymer was purchased from Polymer Source Inc. and used without any further purifications. The number-average molecular weights (M_n) of PS and PnBMA blocks are 45,000 g/mol and 48,000 g/mol, respectively. Hence the mole fraction of PS is 56%. The polydispersity index (PDI) is 1.10, determined by size exclusion chromatography (SEC). The molecular structure of PS-*b*-PnBMA copolymer is confirmed by the ^{1}H NMR spectrum, as illustrated in Figure S7. The full-range thermogram presented in Figure S1 shows that the glass transition temperatures are 105 °C and 59 °C for PS and PnBMA blocks, respectively, denoted by $T_{g,\ PS\ block}$ and $T_{g,\ PnBMA\ block}$. It should be noted that the difference between the T_gs of the two blocks is 46 °C. Such a large difference in T_g provides an adequate space to settle down aging response of the two blocks in separate temperature ranges, to clearly presenting the individual aging response.

The PS homopolymer, denoted by homo-PS, was purchased from Shanghai Ziqibio Co. Ltd. and utilized in control experiments. For a direct comparison, it has a similar M_n of 45,000 g/mol. The PDI of the homo-PS is 1.13, determined by SEC. The T_g of this homo-PS is 107 °C, which is close to the T_g of PS block in the copolymer sample.

2.2 Enthalpy Relaxation Test

A Shimadzu DSC-60 Plus differential scanning calorimeter (DSC) with the environment of nitrogen gas was used to perform enthalpy relaxation experiments, as described in our previous work.[47] In aging testing, a sample of 3-5 mg was sealed in an aluminum pan. The sample

was first heated to 160 °C with a heating rate of 20 °C/min, and was held for 10 min at the end, in order to remove residual stress. To examine aging of the PS block, the sample was subsequently cooled to a T_a, which is at least 11 °C higher than $T_{g,\ \text{PnBMA block}}$ but below the $T_{g,\ \text{PS block}}$, with a constant cooling rate of 30 °C/min. The sample was annealed thereafter for a specific aging time (t_a). After that, the aging response was captured in the second cycle, that is, cooling the sample to −20 °C and reheating to 160 °C, with a constant rate of 20 °C/min. The temperature protocol for aging test was presented in our previous work.[47] From the experiments, heat capacity curves can be obtained for both aged or unaged (without annealing at T_a) samples.

Recovered enthalpy of homo-PS was calculated by the integration of heat capacity deviation between aged and unaged responses over a temperature range from glass state to liquid state, as expressed by Equation (1):

$$\Delta H_a = \int_{T_1}^{T_2} \left(c_{p,\text{aged}}(T) - c_{p,\text{unaged}}(T) \right) dT \quad (1)$$

where $c_{p,\ \text{aged}}$ and $c_{p,\ \text{unaged}}$ are the heat capacity values of aged and unaged homo-PS, respectively. T_1 and T_2 are reference temperatures far below and far above T_g, respectively, at which the heat capacity values of unaged and aged samples are identical. However, the equation used to evaluate enthalpy change of PS block in PS-*b*-PnBMA is different from the classic equation above. The T_a is at least 11 °C higher than $T_{g,\ \text{PnBMA block}}$. As such, it is considered that the aging response of copolymer is merely contributed by the PS block due to thermodynamic equilibrium of PnBMA block. The method of enthalpy calculation introduced in our previous work was used to determine recovered enthalpy of the PS block,[44] as shown in Equation (2):

$$\Delta H_{a,\text{PS block}} = \int_{T_1}^{T_2} \left(c_{p,\text{copolymer,aged}}(T) - c_{p,\text{copolymer,unaged}}(T) \right) \times \frac{M_{\text{copolymer}}}{M_{\text{PS block}}} \mathrm{d}T \quad (2)$$

where $c_{p,\ \text{copolymer,\ aged}}$ and $c_{p,\ \text{copolymer,\ unaged}}$ are the heat capacity of aged and unaged copolymer samples, respectively. $M_{\text{copolymer}}$ and $M_{\text{PS block}}$ are the molecular weights of the entire copolymer chain and the PS block, respectively.

2.3 Morphology and Modulus Measurement

Morphology and modulus measurements were performed on a Bruker Dimension Icon atomic force microscope (AFM) with a heating stage via the Peak Force Quantitative Nanomechanical Mapping (QNM) technique. To prepare AFM samples, PS-*b*-PnBMA was dissolved in chloroform to form a 2 wt% solution. Subsequently, copolymer thin films were fabricated by spin-coating at 800 *rpm* for 50 s on a silica substrate from this solution. The films were then annealed under vacuum at 80 °C overnight to remove residual solvent and stress. Prior to the morphology tests, the films were heated to 160 °C and were held at there for 10 min, which was in accordance with the thermal protocol in enthalpy relaxation test. Moduli of separated microphases in the copolymer samples were then measured by the AFM.

3 Results and Discussion

The heat capacity of PS-*b*-PnBMA diblock copolymer under various T_as are depicted in Figure 1. As a reference, the aging results of homo-PS are illustrated in Figure S2. Apparent heat capacity overshoots of PS block appear in the proximity of $T_{g,\,PS\ block}$ when T_as is relatively high, *i.e.*, 15 °C or 20 °C lower than $T_{g,\,PS\ block}$. In contrast, as T_a is $T_{g,\,PS\ block}$ − 35 °C or $T_{g,\,PS\ block}$ − 30 °C, low and broad c_p overshoots of PS block occur at a temperature range evidently lower than the $T_{g,\,PS\ block}$, whereas homo-PS shows high and narrow heat capacity peaks near its T_g over all T_as in our tests. The aging overshoots of homo-PS at the same temperature departures with respect to $T_{g,\,PS}$ are much higher than that of PS block in PS-*b*-PnBMA. Intriguingly, Boucher and coworkers showed similar low and broad heat capacity curves in freely standing homo-PS nanoconfined films.[1, 32] The aging characteristics above for the PS blocks in PS-*b*-PnBMA is qualitatively in agreement with that of the 95-nm PS thin films demonstrated in Boucher *et al.*'s work.[1] Nevertheless, the peak position and height of PS blocks in this work is obviously lower than those of PS thin films. The details from a direct comparison are summarized in Table 1. In addition to confined PS, bulk PS can also present low and broad

aging overshoots which indicate the fast relaxation mechanism. To detect this behavior, a T_a of T_g − 55 °C and a t_a as long as 260 hrs are required.[48]

Figure 2 shows the ΔH_a of PS block and homo-PS undergone aging at different temperatures.

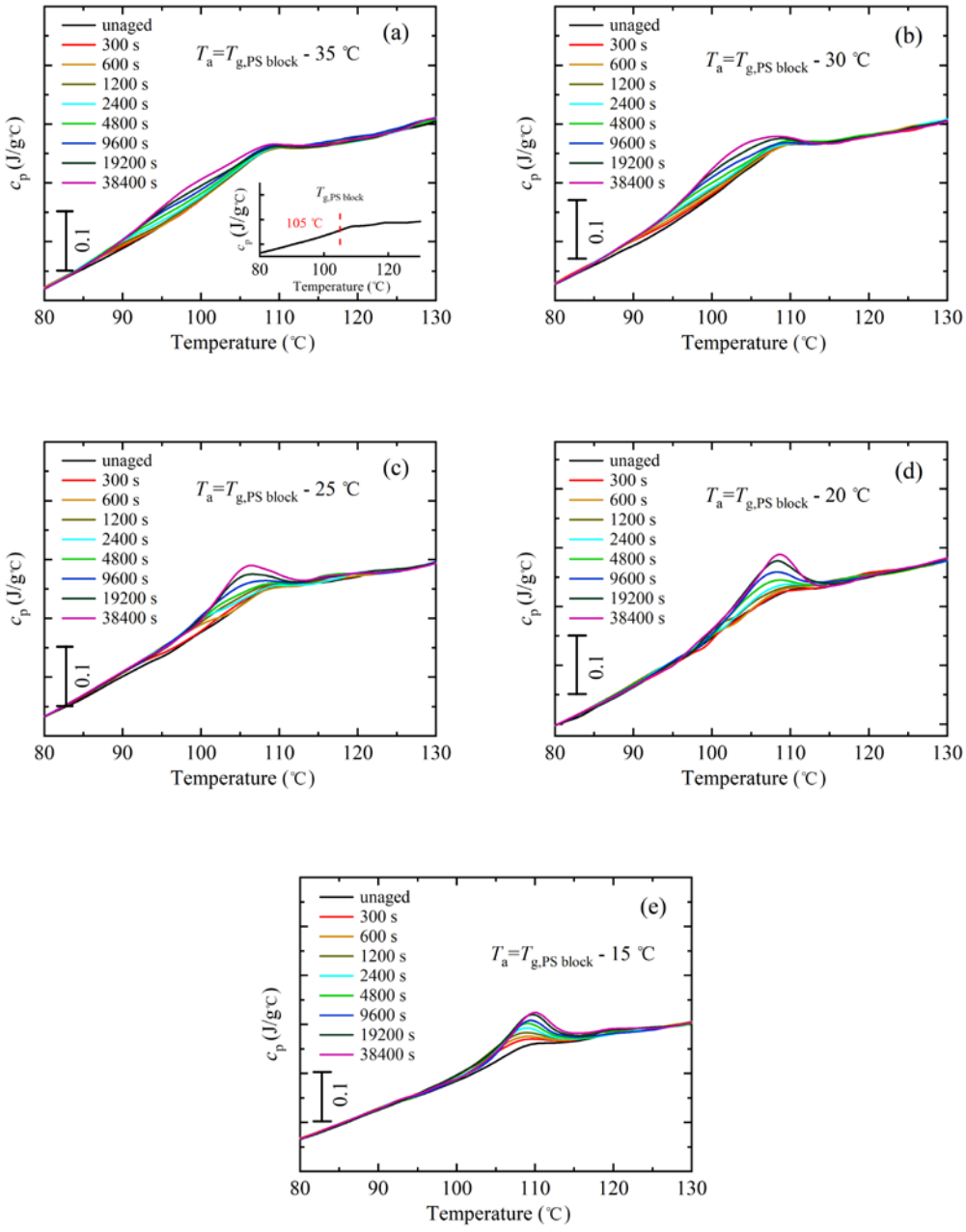

Figure 1. Heat capacity of PS-*b*-PnBMA diblock copolymer. (a) T_a = $T_{g,\ PS\ block}$ − 35 °C, (b) T_a = $T_{g,\ PS\ block}$ − 30 °C, (c) T_a = $T_{g,\ PS\ block}$ − 25 °C, (d) T_a = $T_{g,\ PS\ block}$ − 20 °C, and (e) T_a = $T_{g,\ PS\ block}$ − 15 °C.

The aging rate is defined by the slope of the linear portion of ΔH_a versus logarithmic t_a. At higher T_as, for example, $T_a = T_{g,\,PS} - 15$ °C or $T_{g,\,PS\ block} - 15$ °C, both ΔH_a and aging rate of PS block in PS-*b*-PnBMA are restrained to be lower than those of homo-PS. This result qualitatively matches our previous findings in homo-PMMA and PMMA block in PS-*b*-PMMA diblock copolymer.[44] When aging temperature decreases to $T_{g,\,PS\ block} - 25$ °C, the aging rate of PS block is markedly enhanced and it gets close to the value of homo-PS, however, the relaxed enthalpy of PS block is still less than that of the homo-PS. When aging temperature is equal to or lower than $T_{g,\,PS} - 30$ °C or $T_{g,\,PS\ block} - 30$ °C, the enthalpy change and aging rate of PS block surpass those of the homo-PS. We note that, as indicated by the start point of the fitted lines in Figure 2(a), the relaxed enthalpy of PS block shows a linear dependence on the logarithm of t_a from t_a = 600 s when $T_a = T_{g,\,PS\ block} - 35$ °C. Nevertheless, the homo-PS presents a delayed linear dependence from t_a = 1,200 s under the same condition, meaning weaker and slow loading process of aging for homo-PS at this T_a.

The aging rate as a function of aging temperature is illustrated in Figure 3. In general, the aging rate shows a maximum at an intermediate T_a.[49] The results in Figure 3 implies that the aging speed of PS block under soft confinement exhibits a different dependence on $T_g - T_a$. When T_a is close to T_g, the aging rate of PS block is much reduced, compared to its counterpart of the homopolymer. Nevertheless, the aging rate of PS block increases with decreasing T_a

Table 1. Aging response features of PS block and PS thin films.

Material	Aging temperature (°C)	Aging time (s)	Response regime (°C)	Peak position (°C)	Peak height (J/g°C)
PS block	$T_g - 35$	19,200	$T_g - 22.5$ to $T_g + 13.2$	$T_g - 8.9$	0.029
PS block	$T_g - 35$	38,400	$T_g - 23.0$ to $T_g + 13.2$	$T_g - 7.6$	0.036
PS thin films [a]	$T_g - 36$	28,800	$T_g - 22.5$ to $T_g + 13.2$	$T_g - 1.9$	0.057

[a]The data of PS block in PS-*b*-PnBMA diblock copolymer and 95-nm freely standing PS thin films from Boucher *et al.*[1] are attained from deviated heat capacity ($c_{p,\,aged} - c_{p,\,unaged}$) results, as depicted in Supporting Information.

and even exceeds the aging rate of homo-PS when $T_a < T_g - 30$ °C. These results suggest that the PS block in PS-*b*-PnBMA exhibits a significant difference on the aging rate profile from

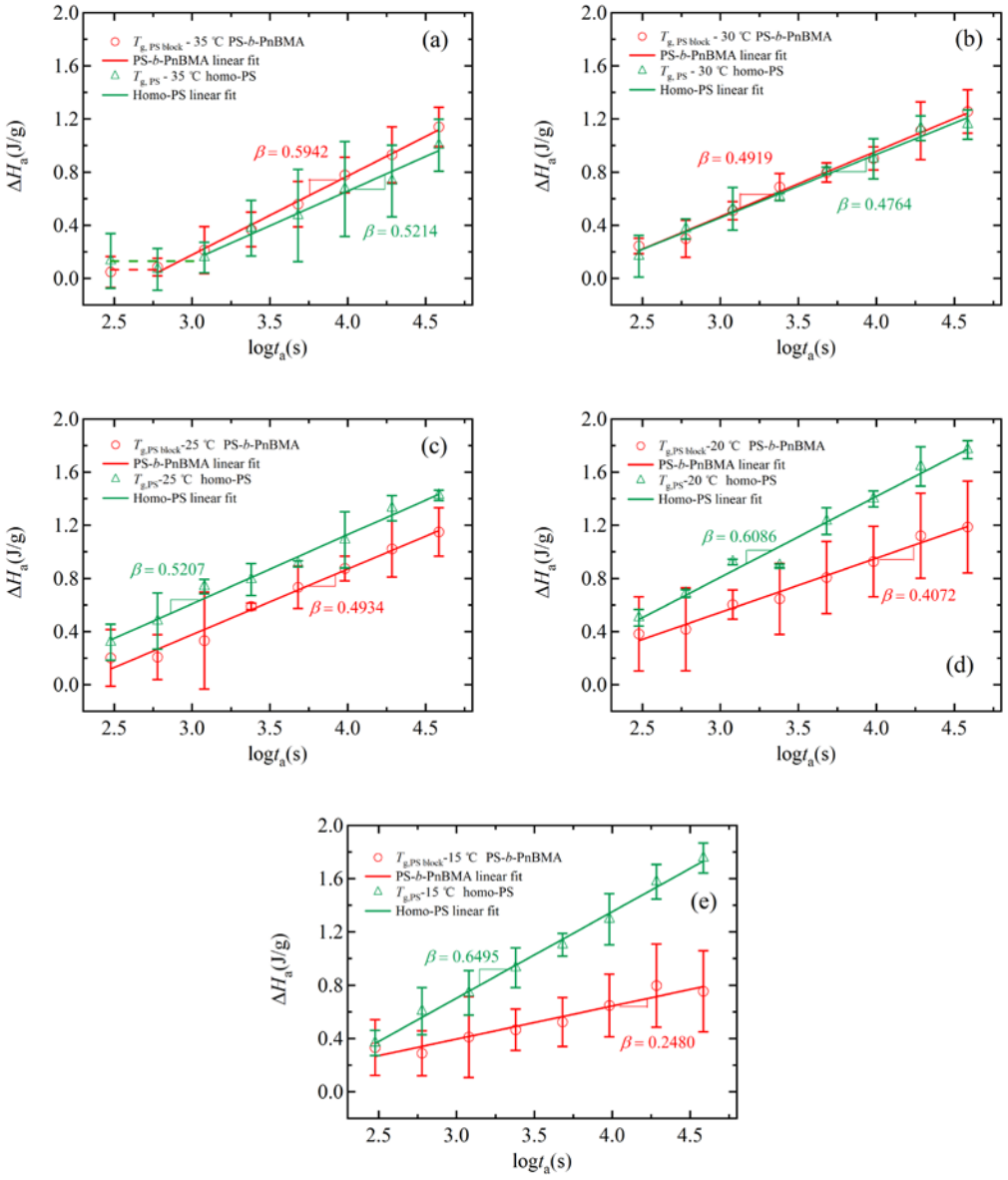

Figure 2. Relaxed enthalpy of PS block in copolymer and corresponding homopolymer. The error bar represents the standard deviation of data of three duplicates, and β is the aging rate from linear fit. (a) $T_a = T_{g,\,PS} - 35$ °C or $T_{g,\,PS\ block} - 35$ °C, the dashed lines are guides for the eyes, (b) $T_a = T_{g,\,PS} - 30$ °C or $T_{g,\,PS\ block} - 30$ °C, (c) $T_a = T_{g,\,PS} - 25$ °C or $T_{g,\,PS\ block} - 25$ °C, (d) $T_a = T_{g,\,PS} - 20$ °C or $T_{g,\,PS\ block} - 20$ °C, and (e) $T_a = T_{g,\,PS} - 15$ °C or $T_{g,\,PS.\,block} - 15$ °C. The data of homo-PS under aging temperature from $T_{g,\,PS} - 35$ °C to $T_{g,\,PS} - 20$ °C are from our previous work.[3]

the homo-PS in our testing range of T_a. The change of soft confinement environment may account for the complicated effect on different aging temperatures. That is, with decreasing T_a closer to $T_{g,\ \text{PnBMA block}}$, PnBMA block no longer constructs strong soft confinement to PS block, making contrary impact on the physical aging of PS block from its effect at higher T_as. To verify this hypothesis, we examine the confinement condition by investigating morphology and modulus of PS-*b*-PnBMA samples.

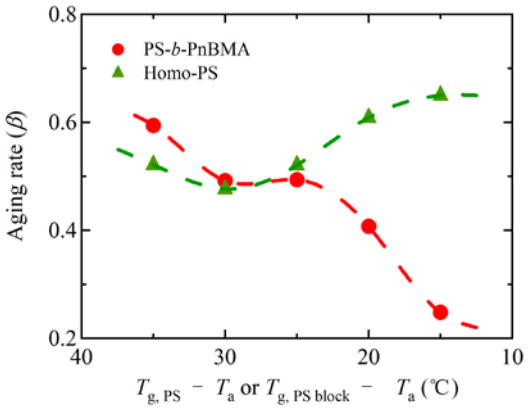

Figure 3. Aging rate of PS-*b*-PnBMA diblock copolymer and the corresponding homo-PS. The dashed lines are guides for the eyes. The data of homo-PS under aging temperature from $T_{g,\ PS}$ – 35 °C to $T_{g,\ PS}$ – 20 °C are from our previous work.[3]

Samples were monitored at two representative temperatures of 70 °C and 90 °C, that are, $T_{g,\ PS\ block}$ − 35 °C (or $T_{g,\ PnBMA\ block}$ + 11 °C) and $T_{g,\ PS\ block}$ − 15 °C (or $T_{g,\ PnBMA\ block}$ + 31 °C), respectively, under the QNM technique of AFM imaging. In order to accurately determine moduli of the microphases, the surface deformation was set to be larger than 2 nm by controlling the applied force in the testing. Figure 4 illustrates AFM modulus images of representative PS-*b*-PnBMA diblock copolymer samples. The bright domains are PS block and the dark domains are PnBMA block, according to their modulus values. The color scales range from 7.0 to 9.1 MPa and 2.0 to 2.7 MPa for 70 °C and 90 °C, respectively. The AFM modulus images of PS-*b*-PnBMA display multiple interconnected domains showing distinct two levels of moduli, which we speculate reflect to the separated PS- and PnBMA-riched phases. In order to confirm our phase separation results, the surface free energy and AFM modulus

measurements were carried out.

The materials on the surface were examined by surface free energy experiment via a Kruss DSA100 contact angle meter. The test liquids were water and diiodomethane. The average contact angles of water and diiodomethane are 89.6 ° and 42.7 °, respectively, as the average values from three duplicates with very small deviations. The representative contact angle images are illustrated in Figure S4. Subsequently, the surface free energy of PS-*b*-PnBMA copolymer thin film was calculated to be 38.6 mN/m by the method introduced by Owens *el al.*[50] Compare this value to those of homo-PS and homo-PnBMA, which are 40.7 mN/m and 31.2 mN/m, respectively,[51] the surface free energy of the copolymer sample is between the values of PS and PnBMA homo-polymers. It indicates that both PS and PnBMA components exist on the surface of our PS-*b*-PnBMA copolymer samples.

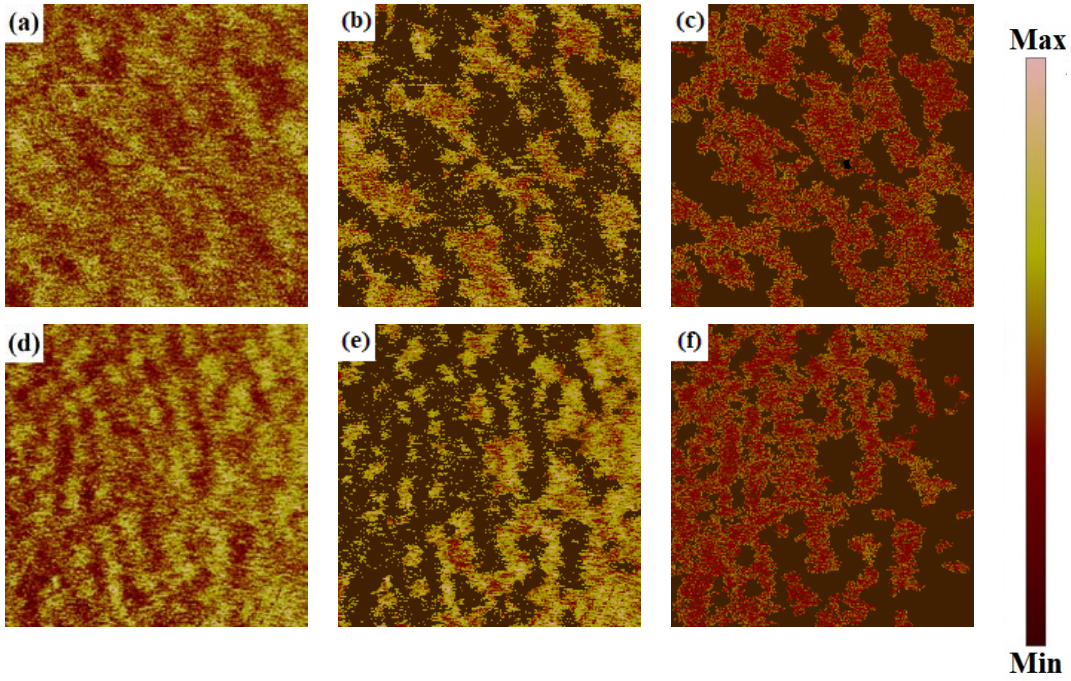

Figure 4. AFM modulus images of PS-*b*-PnBMA diblock copolymer samples at two representative temperatures. (a) overall image at 70 °C, color scale ranges from 7.0 to 9.1 MPa, and (d) overall image at 90 °C, color scale ranges from 2.0 to 2.7 MPa, (b) highlighted (brighter, the same below) PS-riched domains at 70 °C, (c) highlighted PnBMA-riched domains at 70 °C, (e) highlighted PS-riched domains at 90 °C, and (f) highlighted PnBMA-riched domains at 90 °C. Image size: 400 nm × 400 nm.

Modulus of PS-*b*-PnBMA was also detected at 26 °C, as shown in Figure S5. In the modulus image, two types of domains display apparently different moduli and exhibit analogous structure to the AFM results at 70 °C and 90 °C. Together with surface free energy results, it suggests that phase separation results of our PS-*b*-PnBMA are consistent from room temperature to our aging temperatures. We note that Russell and coworkers demonstrated no phase separation detected at around 80 °C in their perdeuterated polystyrene-*block*-poly(n-butyl methacrylate) (PdS-*b*-PnBMA) via small angle X-ray scattering (SAXS) during heating.[52] In addition to the general order-to-disorder transition (ODT), they found that PdS-*b*-PnBMA exhibited a lower disorder-to-order transition (LDOT).[52] That is, the phase separation reformed above ~120 °C in the process of slow heating with a constant rate of 5 °C/min. However, the disordered microstructure in PdS-*b*-PnBMA at 80 °C or less could not be detected during cooling at the same rate, due to the long relaxation time when approaching T_g. Therefore, we do not think that the phase diagram from heating in their work is appropriate for our PS-*b*-PnBMA. We ascribe this mismatch to different thermal histories. The copolymer samples in this work were quenched to the T_as with a cooling rate of 30 °C/min after annealed at 160 °C for 10 min, at where phase separation was established. As the cooling rate was 6 times higher than that in Russell *et al.*'s work, the phase separation should be majorly remained to the aging temperatures below T_g. The AFM modulus images in Figure 4 reflect microphase separation which is fairly stable due to the long relaxation time below T_g.

From image analysis, modulus histograms of phase separated PS-*b*-PnBMA are obtained and displayed in Figure 5. The statistical data of whole sample (black cityscapes) are the sum of the results of the two individual blocks (bars in color). The statistical mean fraction of PS phase in modulus images is 48 %, which is consistent with its mole fraction. As shown in Figure 5, although the distribution functions of two types of microphases are overlapped in an intermediate modulus region, the average modulus of the two blocks are detected, as listed in Table 2. Here the Young's moduli of the homopolymers at corresponding temperatures obtained by dynamic mechanical analysis (DMA) with a frequency of 1 Hz are cited as

references.[2, 16] Owing to the different T_g, the same departure from T_g of homo-PnBMA in the literature is likely not at 70 °C or 90 °C. Note that a direct matchup of T_gs measured by DSC and DMA does not exist, we estimated reasonable intervals of Young's modules of 1.44-14.81 MPa and 0.39-1.42 MPa for $T_{g,\ PnBMA}$ + 11 °C and $T_{g,\ PnBMA}$ + 31 °C, respectively.[16] The modulus values of the PnBMA at these temperatures are higher than those of the homo-PnBMA. We attribute this enhancement to residual PS blocks in the PnBMA-riched phases or a mass of PS blocks in adjacent PS-riched phases served as hard confinement, which is consistent with the findings of enhanced modulus under hard confinement in the literature.[53-55] Furthermore, the covalent bonding between PS and PnBMA blocks restricts the degree of freedom of the PnBMA blocks, likely contributing to the enhanced modulus as well.[56-58] In contrast to the close modulus of PnBMA in copolymer and homopolymer, the modulus of PS block is more than two orders of magnitude lower than the modulus of glassy homo-PS measured at comparable temperatures.[2] Soft confinement constructed by the PnBMA blocks in the vicinity of interfaces somewhat contributes for the reduced modulus of PS block. However, it is not the main reason for this tremendous softening, as the modulus under soft confinement is at most an order of magnitude lower than bulk value when the domain dimension is less than 20 nm.[59-61] AFM modulus image is calculated by deformation. It suggests that the detected deformation of PS-riched domains is substantially contributed by the residual PnBMA blocks due to its low modulus and correspondingly large deformation. With this speculation, the actual deviation between PS and PnBMA domains is much higher than the data shown in Table 2. Together with apparent phase separation of two blocks shown in Figure 4, it is confirmed that the soft confinement for PS block constructed by PnBMA block exists in entire experimental T_a range from $T_{g,\ PS\ block}$ − 35 °C to $T_{g,\ PS\ block}$ − 15 °C. As such, to answer the question why the aging rate of PS block is no longer constrained at low T_as even though soft confinement system is remained, a new mechanism should be proposed.

Referring back to the typically low and broad heat capacity in PS thin films at a low T_a, Boucher and coworkers suggested that PS exhibited two equilibration mechanisms.[1, 32] To support this

point of view, they plotted the T_a-dependent relaxed enthalpy of PS thin films after a fixed aging time.[1, 32] The two local maximums of ΔH_a signify the two mechanisms for structural recovery. Similarly, the relation between ΔH_a and T_a of the PS blocks in PS-*b*-PnBMA after fixed aging times was examined, as shown in Figure 6. Different from a unique local maximum of ΔH_a for homo-PS in the entire T_a regime, recovered enthalpy of PS blocks presents a second local maximum at a lower T_a of ~75 °C. It indicates that the second fast mechanism exists in PS blocks, which corresponds to the T_as on which the low and broad heat capacity curves appear as shown in Figure 1. This feature, in combination with the results of the fast mechanism in

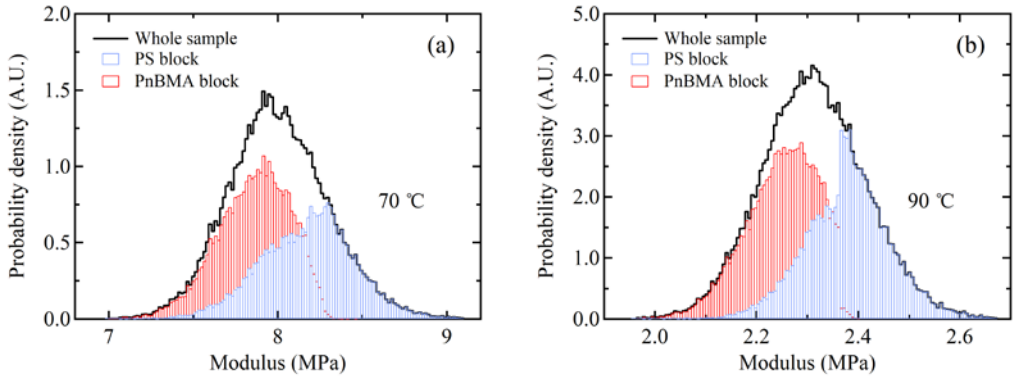

Figure 5. Modulus histograms of PS-*b*-PnBMA diblock copolymer samples at two representative temperatures. The black cityscapes are the modulus of whole sample. The red and blue bars are the statistically distributed modulus of PnBMA block and PS block from AFM results, respectively. The sum of two blocks contribution is equal to the histogram of the whole sample. (a) 70 °C, and (b) 90 °C.

others' work, authenticates that the fast mechanism is active at low temperatures in some polymeric systems.[1, 27, 32] That is, such mechanism is concealed at high T_as due to conspicuous aging response of first equilibration mechanism, whereas when aging at low T_as under weak driving force, the fast mechanism comes to the surface due to its low activation energy. [1, 27, 32] Here, in line with the concept that soft confinement reduces the timescale for the presence of the second equilibration,[1, 32-33] we report an analogous timescale shortening effect (fast mechanism appears within 38,400 s) under soft confinement in a block copolymer. Together

with suppressed aging at high T_as, it is supposed that soft confinement effect can be considered as a competition between aging constrained effect and timescale shortening effect on the second equilibration mechanism. At higher T_as, the second equilibration mechanism is hidden due to strong driving force of the ordinary aging. Hence, soft confinement effect is dominated by aging constrained effect, resulting in suppressed aging rate of PS block in PS-*b*-PnBMA. With decreasing T_a, timescale shortening effect plays a more important role and the second mechanism emerges on a short timescale, inducing enhanced aging rate of PS block. The timescale shortening effect can be successfully described by the free volume holes diffusion model.[1] The hole diffusion coefficient of free volume holes and the shift factor of the equilibrium time of the fast mechanism are in inverse proportion.[1] In other words, the equilibrium time of the fast mechanism becomes shorter for the material system with larger free interface fraction. Correspondingly, we think the free volume holes diffusion model can explain the timescale shortening effect in our copolymer. A large number of interfaces between PS and PnBMA block formed by phase separation initiate the recovery process and increase the hole diffusion coefficient compared to that in bulk PS. As such, the timescale of the fast mechanism is shortened in our copolymer.

Table 2. Moduli of the two phases and corresponding homopolymers at representative aging temperatures.

Sample	Modulus at 70 °C[a] (MPa)	Modulus at 90 °C[b] (MPa)
PS-riched phase	8.17	2.38
PnBMA-riched phase	7.85	2.25
Homo-PS[c]	≈ 2000	≈ 2000
Homo-PnBMA[d]	2.72	0.52

[a] $T_{g,\ PS\ block} - 35$ °C or $T_{g,\ PnBMA\ block} + 11$ °C.

[b] $T_{g,\ PS\ block} - 15$ °C or $T_{g,\ PnBMA\ block} + 31$ °C.

[c] Bulk PS measured by DMA from Spinks *et al.*[2]

[d] PnBMA latex film measured by DMA from Choi *et al.*[16] The lower bounds and upper bounds are obtained when the T_g is defined by the peak temperature of damping curve and the extrapolated onset of storage modulus, respectively.

In the vicinity of the interface with the PnBMA domains, the PS chain segments possess enhanced mobility due to the soft confinement effect. The mobility decreases with increasing distance from the interface, exhibiting a gradient change to the interior of the PS domain. Under this circumstance, a two-layer model containing stepwise mobility levels, is often utilized to equivalently describe the effect of the enhanced mobility on T_g or chain dynamics,[62] as shown in Figure S6. The higher level of mobility accounts for the enhanced mobility, whereas the lower mobility corresponds the bulk value. As the T_g of the PS domains is quite close to the bulk T_g, we believe the influence of the enhanced mobility due to the interaction with PnBMA only exists within a small range, resulting in no apparent deviation of the T_g of PS domains from the bulk. This unique characteristic could be attributed to the direct connection of the two blocks through covalent bonding. In the two-layer model depicted in Figure S6, the effect of the extreme thin layer of PS with high mobility on physical aging is much weaker than that from the massive bulk-like PS chains. Thus we believe the gradient of mobility of PS is not the reason for the presence of two equilibrations. This speculation is in line with the results in the literature showing the coexistence of two structural recovery mechanisms in bulk PS.[27]

Several works studied the kinetics of two equilibrium recovery in confined polymers.[1, 33-34] Cangialosi and coworkers found that the slow mechanism obeys super-Arrhenius temperature dependence, which associates with α transition, whereas the fast mechanism displays Arrhenius temperature dependence.[1, 33-34] Analogous results were reported in a metallic glass by Monnier *et al.*[63] They found that vitrification exhibits different temperature dependence in α relaxation. These results demonstrate the decoupling between vitrification and α relaxation in glasses. As our copolymer shows similar aging characteristics to that of confined polymers, we hypothesize that the decoupling is also exists in our copolymer. That is, the fast mechanism originates from a class of specific chain motions, which are not involved in α relaxation. This will be checked in further work by investigating the temperature dependence

of the time to reach equilibrium.

For a direct comparison of two soft confinement systems, ΔH_a values of PS thin films aged for 28,800 s, as a function of aging temperature, are included in Figure 6.[1] The characteristics of recovered enthalpy in two systems, namely PS-*b*-PnBMA block copolymer and PS thin film, are quantitatively inconsistent. Two local maximums and one local minimum inbetween, *i.e.*, the saddle-shaped curve as reported in literature,[1, 32-33] of the ΔH_a of PS block, locate in a small temperature regime (T_g – 35 °C to T_g – 15 °C), whereas the same feature of PS thin films distribute in a very large temperature regime (T_g – 135 °C to T_g – 5 °C, the whole temperature regime is not presented in Figure 6).[1] Apart from the different molecular weight (the weight-average molecular weight of PS in Boucher's work is 1, 408, 000 g/mol)[1], the major reason for these disagreement might be confinement condition. Soft confinement in PS thin films is constructed by free surface, which is mostly influenced by film thickness rather than temperature. In vicinity of the free surface it possesses very high mobilities even at ambient temperature. In contrast to the steady confinement condition over temperatures in freely standing films, confinement intensity in our block copolymers, which is characterized by the modulus of PnBMA block, possesses pronounced temperature dependence. As shown by modulus analysis at different temperatures, the modulus of PnBMA block dramatically increases with decreasing T_a, resulting in markedly reduced confinement intensity and consequently weakening timescale shortening effect on the second equilibration mechanism. The second local minimum of ΔH_a for PS block emerges in the temperature regime from T_g – 35 °C to T_g – 25 °C, at temperatures higher than that in PS thin films.[1] Another thing should be noticed is that the tendency of ΔH_a in PS thin films is identical to that of homo-PS, monotonously decreasing with similar slope in the temperature regime from T_g – 15 °C to T_g – 30 °C, especially for 95-nm PS thin films, even though the value of ΔH_a is aberrant. However, the tendency in PS blocks is considerably different, showing saddle-shaped curve in this temperature regime. The value of ΔH_a in PS blocks is close to the counterpart of homo-PS over T_g – 30 °C to T_g – 35 °C, whereas PS thin films contain a local minimum over same

temperature regime. The outcome of this comparison provides a further confirmation that confinement intensity in copolymer is declined at lower T_as.

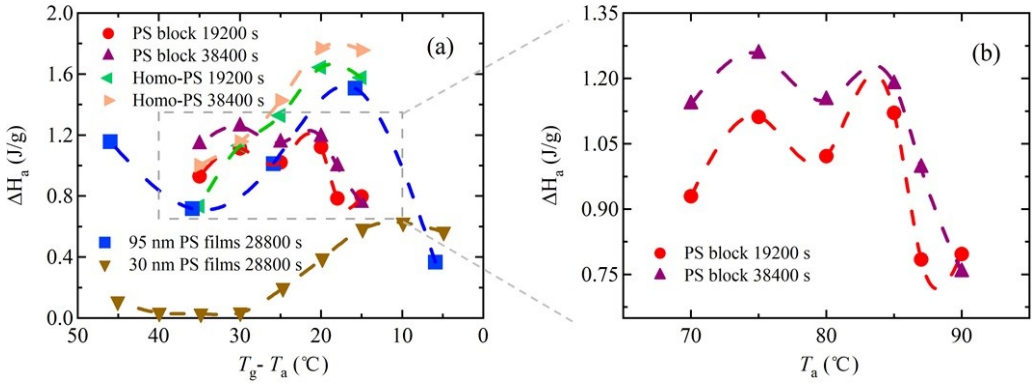

Figure 6. (a) Recovered enthalpy as a function of aging temperature after a constant aging time. PS block after aging 19,200 s (●), PS block after aging 38,400 s (▲), homo-PS after aging 19,200 s (◂), Homo-PS after aging 38,400 s (▸), 95-nm PS thin films after aging 28,800 s (480 min) from Boucher *et al.*[1] (■), and 30-nm PS thin films after aging 28,800 s (480 min) from Boucher *et al.*[1] (▼). The dash lines are guides for the eyes. (b) Recovered enthalpy of PS blocks in PS-*b*-PnBMA, enlarged from the area delimited by the gray dashed lines.

We notice that the T_g of PnBMA block in our copolymer samples is 59 °C, which is evidently enhanced from the T_g result of homo-PnBMA (20 °C ~ 31 °C) reported in other works.[64-65] We believe this large departure can be attributed to hard confinement from PS blocks under microphase separation. Similarly, Baglay and coworkers found that the local T_g of homo-PnBMA 25 nm away from the interface with a PS underlayer is 15 °C higher than that of the bulk.[64, 66] In our PS-*b*-PnBMA copolymer, the thickness of PnBMA-riched domain is also around 25 nm, as shown in Figure 4. Here the hard confinement for PnBMA domain is provided by PS-riched domains from both sides rather than one side in Baglay *et al.*'s work. In addition, the covalent bond between two blocks further constrains the mobility of PnBMA block. As such, we speculate that the hard confinement effect on T_g enhancement in our copolymer is even stronger than that in Baglay *et al.*'s work, and this hard confinement results in the approximate 30 °C increase of T_g of the PnBMA block. Such large enhancement is

definitely worth a quantitative demonstration in future studies.

4. Conclusions

Three-dimensional soft confinement manifests complicated effects on physical aging of PS blocks in PS-*b*-PnBMA under microphase separation. When T_a is equal or greater than $T_{g,\,PS\,block} - 25$ °C, aging of PS blocks is restrained as demonstrated by lower heat capacity overshoots and a reduced aging rate. In contrast, aging rate of PS blocks is enhanced at lower T_as because of the appearance of a second equilibration process. Morphology examination reveals that soft confinement exerts on PS-riched domains over the entire T_a regime, which does not support the viewpoint that the complicated confinement effect is attributed to vanish of soft confinement at low T_as. Two local maximums of ΔH_a versus T_a suggest that two equilibrations coexist during aging of PS blocks. With these results, it is concluded that soft confinement restrains aging at high aging temperatures, but significantly shortens the timescale of appearance of the second and fast structural relaxation process at low T_as, resulting in a low and broad c_p response and an enhanced aging rate.

AUTHOR INFORMATION

Corresponding Author

*E-mail: yunlong.guo@sjtu.edu.cn

Notes

The authors declare no competing financial interest.

ACKNOWLEDGMENT

The authors acknowledge the National Science Foundation of China for financial support through the General Program 2157408.

SUPPORTING INFORMATION

Full-range thermogram, heat capacity of homo-PS, deviated heat capacity results, contact angle results, and modulus image.

REFERENCES

1. Boucher, V. M.; Cangialosi, D.; Alegría, A., Complex nonequilibrium dynamics of stacked polystyrene films deep in the glassy state. *J. Chem. Phys.* **2017,** *146*, 203312.
2. Spinks, G. M.; Brown, H. R.; Liu, Z., Indentation testing of polystyrene through the glass transition. *Polym. Test.* **2006,** *25*, 868–872.
3. Ma, M.; Guo, Y., Accelerated Aging of PS Blocks in PS-*b*-PMMA Diblock Copolymer under Hard Confinement. *J. Phys. Chem. B* **2019,** *123*, 2448–2453.
4. Brennan, A. B.; Feller, F., Physical aging behavior of a poly(arylene etherimide). *J. Rheol.* **1995,** *39*, 453–470.
5. Odegard, G. M.; Bandyopadhyay, A., Physical Aging of Epoxy Polymers and Their Composites. *J. Polym. Sci. Pol. Phys.* **2011,** *49*, 1695–1716.
6. Soloukhin, V. A.; Brokken-Zijp, J. M.; Asselen, O. L. J. v.; With, G. d., Physical Aging of Polycarbonate: Elastic Modulus, Hardness, Creep, Endothermic Peak, Molecular Weight Distribution, and Infrared Data. *Macromolecules* **2003,** *36*, 7585–7597.
7. Pan, P.; Zhu, B.; Inoue, Y., Enthalpy Relaxation and Embrittlement of Poly(L-lactide) during Physical Aging. *Macromolecules* **2007,** *40*, 9664–9671.
8. Cowie, J. M. G.; Ferguson, R., Physical Aging Studies in Poly (vinyl methyl ether). 1. Enthalpy Relaxation as a Function of Aging Temperature. *Macromolecules* **1989,** *22*, 2307–2312.
9. Hutchinson, J. M.; S. Smith; Horne, B.; Gourlay, G. M., Physical Aging of Polycarbonate: Enthalpy Relaxation, Creep Response, and Yielding Behavior. *Macromolecules* **1999,** *32*, 5046–5061.
10. Huang, Y.; Paul, D. R., Effect of Film Thickness on the Gas-Permeation Characteristics of Glassy Polymer Membranes. *Ind. Eng. Chem. Res.* **2007,** *46*, 2342–2347.
11. Murphy, T. M.; Langhe, D. S.; Ponting, M.; Baer, E.; Freeman, B. D.; Paul, D. R., Physical aging of layered glassy polymer films via gas permeability tracking. *Polymer* **2011,** *52*, 6117–6125.
12. Rowe, B. W.; Freeman, B. D.; Paul, D. R., Physical aging of ultrathin glassy polymer films tracked by gas permeability. *Polymer* **2009,** *50*, 5565–5575.
13. Boucher, V. M.; Cangialosi, D.; Alegría, A.; Colmenero, J.; González-Irun, J.; Liz-Marzan, L. M., Accelerated physical aging in PMMA/silica nanocomposites. *Soft Matter* **2010,** *6*, 3306–3317.
14. Priestley, R. D.; Rittigstein, P.; Broadbelt, L. J.; Fukao, K.; Torkelson, J. M., Evidence for the molecular-scale origin of the suppression of physical ageing in

confined polymer: fluorescence and dielectric spectroscopy studies of polymer–silica nanocomposites. *J. Phys.: Condens. Matter* **2007,** *19*, 205120.
15. Alegría, A.; Goitiandía, L.; Telleriía, I.; Colmenero, J., α-Relaxation in the Glass-Transition Range of Amorphous Polymers. 2. Influence of Physical Aging on the Dielectric Relaxation. *Macromolecules* **1997,** *30*, 3881–3887.
16. Choi, H.-y.; Lee, D.-y.; Lee, J.-y.; Kim, J.-h., Miscibility Behavior of Poly(n-butyl Methacrylate) Latex Films Containing Alkali-Soluble Resin. *J. Appl. Polym. Sci.* **2000,** *78*, 639–649.
17. Hutchinson, J. M., Physical Aging of Polymers. *Prog. Polym. Sci.* **1995,** *20*, 703–760.
18. Hodge, I. M., Physical Aging in Polymer Glasses. *Science* **1995,** *267*, 1945–1947.
19. Struik, L. C. E., Physical Aging in Plastics and Other Glassy Materials. *Polym. Eng. Sci.* **1977,** *17*, 165–173.
20. Cangialosi, D.; Alegría, A.; Colmenero, J., Effect of nanostructure on the thermal glass transition andphysical aging in polymer materials. *Prog. Polym. Sci.* **2016,** *54–55*, 128–147.
21. Huang, Y.; Paul, D. R., Experimental methods for tracking physical aging of thin glassy polymer films by gas permeation. *J. Membrane. Sci.* **2004,** *244*, 167–178.
22. Micoulaut, M., Relaxation and physical aging in network glasses: a review. *Rep. Prog. Phys.* **2016,** *79*, 066504.
23. Boucher, V. M.; Cangialosi, D.; Alegría, A.; Colmenero, J., Enthalpy Recovery of Glassy Polymers: Dramatic Deviations from the Extrapolated Liquidlike Behavior. *Macromolecules* **2011,** *44*, 8333–8342.
24. Cameron, N. R.; Cowie, J. M. G.; R. Ferguson, I. M., Enthalpy relaxation of styrene-maleic anhydride (SMA) copolymers Part 1. Single component systems. *Polymer* **2000,** *41*, 7255–7262.
25. Cowie, J. M. G.; Harris, S.; McEwen, I. J., Physical Ageing in Poly(vinyl Acetate) 1. Enthalpy Relaxation. *J. Polym. Sci. Pol. Phys.* **1997,** *35*, 1107–1116.
26. Pye, J. E.; Roth, C. B., Two Simultaneous Mechanisms Causing Glass Transition Temperature Reductions in High MolecularWeight Freestanding Polymer Films as Measured by Transmission Ellipsometry. *Phys. Rev. Lett.* **2011,** *107*, 235701.
27. Cangialosi, D.; Boucher, V. M.; Alegría, A.; Colmenero, J., Direct Evidence of Two Equilibration Mechanisms in Glassy Polymers. *Phys. Rev. Lett.* **2013,** *111*, 095701.
28. Gallino, I.; Cangialosi, D.; Evenson, Z.; Schmitt, L.; Hechler, S.; Stolpe, M.; Ruta, B., Hierarchical aging pathways and reversible fragile-to-strong transition upon annealing of a metallic glass former. *Acta Mater.* **2018,** *144*, 400–410.
29. Luo, P.; Wen, P.; Bai, H. Y.; Ruta, B.; Wang, W. H., Relaxation Decoupling in Metallic Glasses at Low Temperatures. *Phys. Rev. Lett.* **2017,** *118*, 225901.
30. Golovchak, R.; Kozdras, A.; Balitska, V.; Shpotyuk, O., Step-wise kinetics of natural physical ageing in arsenic selenide glasses. *J. Phys.: Condens. Matter* **2012,** *24*, 505106.

31. Koh, Y. P.; Simon, S. L., Enthalpy Recovery of Polystyrene: Does a Long-Term Aging Plateau Exist? *Macromolecules* **2013,** *46*, 5815–5821.
32. Boucher, V. M.; Cangialosi, D.; Alegría, A.; Colmenero, J., Reaching the ideal glass transition by aging polymer films. *Phys. Chem. Chem. Phys.* **2017,** *19*, 961–965.
33. Perez-De-Eulate, N. G.; Cangialosi, D., Double Mechanism for Structural Recovery of Polystyrene Nanospheres. *Macromolecules* **2018,** *51*, 3299–3307.
34. Monnier, X.; Cangialosi, D., Thermodynamic Ultrastability of a Polymer Glass Confined at the Micrometer Length Scale. *Phys. Rev. Lett.* **2018,** *121*, 137801.
35. Dai, H.; Chen, Q.; Qin, H.; Guan, Y.; Shen, D.; Hua, Y.; Tang, Y.; Xu, J., A Temperature-Responsive Copolymer Hydrogel in Controlled Drug Delivery. *Macromolecules* **2006,** *39*, 6584–6589.
36. Cerritelli, S.; Velluto, D.; Hubbell, J. A., PEG-SS-PPS: Reduction-Sensitive Disulfide Block Copolymer Vesicles for Intracellular Drug Delivery. *Biomacromolecules* **2007,** *8*, 1966–1972.
37. Ranquin, A.; Versées, W.; Meier, W.; Steyaert, J.; Gelder, P. V., Therapeutic Nanoreactors: Combining Chemistry and Biology in a Novel Triblock Copolymer Drug Delivery System. *Nano Lett.* **2005,** *5*, 2220–2224.
38. Grieco, C.; Aplan, M. P.; Rimshaw, A.; Lee, Y.; Le, T. P.; Zhang, W.; Wang, Q.; Milner, S. T.; Gomez, E. D.; Asbury, J. B., Molecular Rectification in Conjugated Block Copolymer Photovoltaics. *J. Phys. Chem. C* **2016,** *120*, 6978–6988.
39. Guo, C.; Lin, Y.-H.; Witman, M. D.; Smith, K. A.; Wang, C.; Hexemer, A.; Strzalka, J.; Gomez, E. D.; Verduzco, R., Conjugated Block Copolymer Photovoltaics with near 3% Efficiency through Microphase Separation. *Nano Lett.* **2013,** *13*, 2957–2963.
40. Mulherin, R. C.; Jung, S.; Huettner, S.; Johnson, K.; Kohn, P.; Sommer, M.; Allard, S.; Scherf, U.; Greenham, N. C., Ternary Photovoltaic Blends Incorporating an All-Conjugated Donor–Acceptor Diblock Copolymer. *Nano Lett.* **2011,** *11*, 4846–4851.
41. Bang, J.; Jeong, U.; Ryu, D. Y.; Russell, T. P.; Hawker, C. J., Block Copolymer Nanolithography: Translation of Molecular Level Control to Nanoscale Patterns. *Adv. Mater.* **2009,** *21*, 4769–4792.
42. Glass, R.; MartinMöller; Spatz, J. P., Block copolymer micelle nanolithography. *Nanotechnology* **2003,** *14*, 1153–1160.
43. Stoykovich, M. P.; Kang, H.; Daoulas, K. C.; Liu, G.; Liu, C.-C.; Pablo, J. J. d.; Müller, M.; Nealey, P. F., Directed Self-Assembly of Block Copolymers for Nanolithography: Fabrication of Isolated Features and Essential Integrated Circuit Geometries. *ACS Nano* **2007,** *1*, 168–175.
44. Ma, M.; Huang, Y.; Guo, Y., Enthalpy Relaxation and Morphology Evolution in Polystyrene-*b*- poly(methyl methacrylate) Diblock Copolymer. *Macromolecules* **2018,** *51*, 7368–7376.
45. Boissé, S. p.; Kryuchkov, M. A.; Tien, N.-D.; Bazuin, C. G. r.; Prud'homme, R. E., PLLA Crystallization in Linear AB and BAB Copolymers of L- Lactide and 2-Dimethylaminoethyl Methacrylate. *Macromolecules* **2016,** *49*, 6973–6986.

46. Gan, Z.; Jiang, B.; Zhang, J., Poly(ε-caprolactone)/Poly(ethylene oxide) Diblock Copolymer. 1. Isothermal Crystallization and Melting Behavior. *J. Appl. Polym. Sci.* **1996,** *59*, 961–967.
47. Ma, M.; Xue, T.; Chen, S.; Guo, Y.; Chen, Y.; Liu, H., Features of Structural Relaxation in Diblock Copolymers. *Polym. Test.* **2017,** *60*, 1–5.
48. Hodge, I. M.; Huvard, G. S., Effects of Annealing and Prior History on Enthalpy Relaxation in Glassy Polymers. 3. Experimental and Modeling Studies of Polystyrene. *Macromolecules* **1983,** *16*, 371–375.
49. Greiner, R.; Schwarzl, F. R., Thermal contraction and volume relaxation of amorphous polymers. *Rheol. Acta* **1984,** *23*, 378–395.
50. Owens, D. K.; Wendt, R. C., Estimation of the Surface Free Energy of Polymers. *J. Appl. Polym. Sci.* **1969,** *13*, 1741–1747.
51. Chen, C.; Wang, J.; Woodcock, S. E.; Chen, Z., Surface Morphology and Molecular Chemical Structure of Poly(n-butyl methacrylate)/Polystyrene Blend Studied by Atomic Force Microscopy (AFM) and Sum Frequency Generation (SFG) Vibrational Spectroscopy. *Langmuir* **2002,** *18*, 1302–1309.
52. Russell, T. P.; Karis, T. E.; Gallot, Y.; Mayes, A. M., A lower critical ordering transition in a diblock copolymer melt. *Nature* **1994,** *368*, 729–731.
53. Cheng, X.; Putz, K. W.; Wood, C. D.; Brinson, L. C., Characterization of Local Elastic Modulus in Confined Polymer Films via AFM Indentation. *Macromol. Rapid Commun.* **2015,** *36*, 391–397.
54. Li, L.; Alsharif, N.; Brown, K. A., Confinement-Induced Stiffening of Elastomer Thin Films. *J. Phys. Chem. B* **2018,** *122*, 10767–10773.
55. Askar, S.; Torkelson, J. M., Stiffness of thin, supported polystyrene films: Free-surface, substrate, and confinement effects characterized via self-referencing fluorescence. *Polymer* **2016,** *99*, 417–426.
56. Lin, Y.; Jin, J.; Song, M., Preparation and characterisation of covalent polymer functionalized graphene oxide. *J. Mater. Chem.* **2011,** *21*, 3455–3461.
57. Zhu, J.; Peng, H.; Rodriguez-Macias, F.; Margrave, J. L.; Khabashesku, V. N.; Imam, A. M.; Lozano, K.; Barrera, E. V., Reinforcing Epoxy Polymer Composites Through Covalent Integration of Functionalized Nanotubes. *Adv. Funct. Mater.* **2004,** *14*, 643–648.
58. Moniruzzaman, M.; Du, F.; Romero, N.; Winey, K. I., Increased flexural modulus and strength in SWNT/epoxy composites by a new fabrication method. *Polymer* **2006,** *47*, 293–298.
59. Torres, J. M.; Stafford, C. M.; Vogt, B. D., Elastic Modulus of Amorphous Polymer Thin Films: Relationship to the Glass Transition Temperature. *ACS Nano* **2009,** *3*, 2677–2685.
60. Stafford, C. M.; Vogt, B. D.; Harrison, C.; Julthongpiput, D.; Huang, R., Elastic Moduli of Ultrathin Amorphous Polymer Films. *Macromolecules* **2006,** *39*, 5095–5099.

61. Liu, Y.; Chen, Y.-C.; Hutchens, S.; Lawrence, J.; Emrick, T.; Crosby, A. J., Directly Measuring the Complete Stress–Strain Response of Ultrathin Polymer Films. *Macromolecules* **2015,** *48*, 6534–6540.
62. Yang, Z.; Fujii, Y.; Lee, F. K.; Lam, C.-H.; Tsui, O. K. C., Glass Transition Dynamics and Surface Layer Mobility in Unentangled Polystyrene Films. *Science* **2010,** *328*, 1676–1679.
63. Monnier, X.; Cangialosi, D.; Ruta, B.; Busch, R.; Gallino, I., Vitrification decoupling from α-relaxation in a metallic glass. *Sci. Adv.* **2020,** *6*, 1454.
64. Baglay, R. R.; Roth, C. B., Communication: Experimentally determined profile of local glass transition temperature across a glassy-rubbery polymer interface with a Tg difference of 80 K. *J. Chem. Phys.* **2015,** *143*, 111101.
65. Kahle, S.; Korus, J.; Hempel, E.; Unger, R.; Höring, S.; Schröter, K.; Donth, E., Glass-Transition Cooperativity Onset in a Series of Random Copolymers Poly(n-butyl methacrylate-stat-styrene). *Macromolecules* **1997,** *30*, 7214–7223.
66. Baglay, R. R.; Roth, C. B., Local glass transition temperature $T_g(z)$ of polystyrene next to different polymers: Hard vs. soft confinement. *J. Chem. Phys.* **2017,** *146*, 203307.

Physical Aging of PS Blocks under 3D Soft Confinement in PS-*b*-PnBMA Diblock Copolymer: Two Equilibrations on The Way

Mingchao Ma[1] and Yunlong Guo*[,1,2]

[1]University of Michigan – Shanghai Jiao Tong University Joint Institute, and [2]School of Materials Science and Engineering, Shanghai Jiao Tong University, Shanghai 200240, China

*Corresponding author, E-mail: yunlong.guo@sjtu.edu.cn

Graphical Abstract

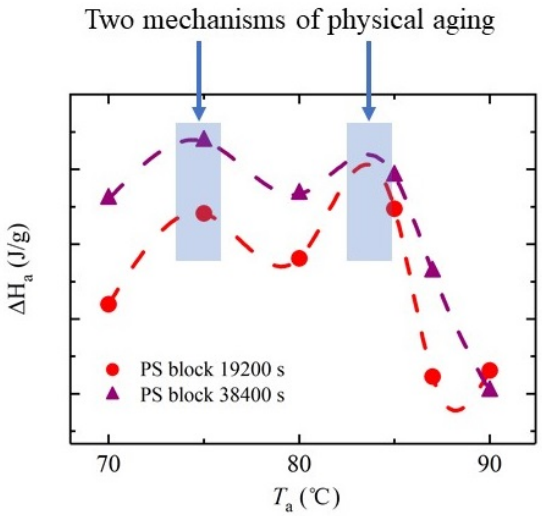

Two local maximums of T_a-dependent ΔH_a of PS block in PS-*b*-PnBMA indicate two relaxation mechanisms during physical aging.